

Conductive Shape Memory Nanocomposites for High Speed Electrical Actuation

Xiaofan Luo and Patrick T. Mather*

Supporting Information

Experimental Methods

Electrospinning and Pyrolysis of Poly(acrylonitrile) (PAN): The solution for electrospinning was prepared by dissolving 1 g PAN ($M_w \sim 150,000$ g/mol from Scientific Polymer Products, Inc.) in 10 ml dimethylformamide (DMF). The electrospinning was conducted using a custom-built setup that consists of a high voltage power supply (Agilent E3630A), a syringe pump (KD Scientific) and a rotating drum collector. The conditions of electrospinning are listed below:

Tip – Collector Distance (cm)	Voltage (kV)	Flow Rate (ml/hr)	Collector Rotating Speed (rpm)
12	12.5	1	400

The as-spun PAN fiber mat was kept in a vacuum oven at room temperature overnight, then at 50 °C for 2 h, and finally at 70 °C for 2 h to ensure complete removal of DMF. The dried fiber mat was pyrolyzed via a two-step process. The first step (stabilization) involved heating the fiber mat in a convection oven (Fisher Isotemp 825F) to 280 °C at 2 °C/min, followed by an isothermal hold for 3 h under air environment. In the second step (carbonization), the stabilized fiber mat was placed in a tube furnace (Eurotherm Carbolite) under constant nitrogen purge (80 ml/min), heated from room temperature to 1000 °C and then kept isothermal at 1000 °C for 1 h.

Composite Fabrication: All the chemicals used were purchased from Sigma-Aldrich, Inc. and used as received. Diglycidyl ether of bisphenol-A (DGEBA) was first preheated at 70 °C. The other resin components, including poly(propylene glycol)bis(2-aminopropyl) ether (Jeffamine D230) and neopentyl glycol diglycidyl ether (NGDE), were added and quickly mixed by

vigorous manual stirring with a glass rod (~ 1 min) until a clear, colorless and low-viscosity mixture was obtained. A piece of CNF mat was then submerged in the resin mixture and maintained there for 10 min. After removing the extra resin on the surfaces, the impregnated CNF mat was sandwiched between two Teflon-covered glass slides with a Teflon spacer, clamped together by two binder clips. The thickness of the Teflon spacer was slightly smaller than that of the CNF mat; therefore a constant compression was applied on the CNF mat. The system was cured in this condition in a convection oven at 100 °C for 1.5 h and post-cured without dimensional constraint at 130 °C for 1 h^[21].

Morphological Characterization: The morphologies of as-spun PAN mat, stabilized PAN mat, carbonized PAN (CNF) mat and Epoxy/CNF composite were characterized by scanning electron microscopy. Samples (except the CNF mat) were sputter coated with gold and examined using a JEOL JSM5600 SEM instrument. An accelerating voltage of 18 kV was used. Each SEM image was evenly divided into 9 sub-images. For each sub-image, 10 fibers were randomly picked and their diameters measured using the ImageJ image analysis program. Therefore, for each sample 90 fibers were measured and the results used to generate the histograms.

Dynamic Mechanical Analysis (DMA): The thermomechanical properties of Epoxy/CNF composites were characterized using DMA. In each case, a rectangular film was loaded under tension and an oscillatory deformation with an amplitude of 10 μm, a frequency of 1 Hz and a “force track” (ratio of static to dynamic force) of 108% was applied. The temperature was then ramped from -30 °C to 150 °C at a linear rate of 3 °C/min. The tensile storage modulus, loss modulus and tangent delta were recorded by the instrument.

Electrically Triggered Shape Recovery Experiment: The electrical resistance, r , of a rectangular nanocomposite film was first measured by a standard four-probe method using a precision

multimeter (FLUKE 8848A). The electrical resistivity (ρ) and conductivity (σ) were calculated as:

$$\rho = r \frac{A}{l} \text{ and } \sigma = \frac{1}{\rho}$$

where A and l are the cross-sectional area and distance between two electrodes, respectively. The electrically triggered shape recovery experiment was conducted using a “II” shaped geometry and a DC power supply (Micronta 0-24 V variable power supply). Digital images were taken using a digital camera (Nikon FinePix S9100) at a constant frame rate of 30 Hz and with the sample imaged from the side to visualize the sample curvature.

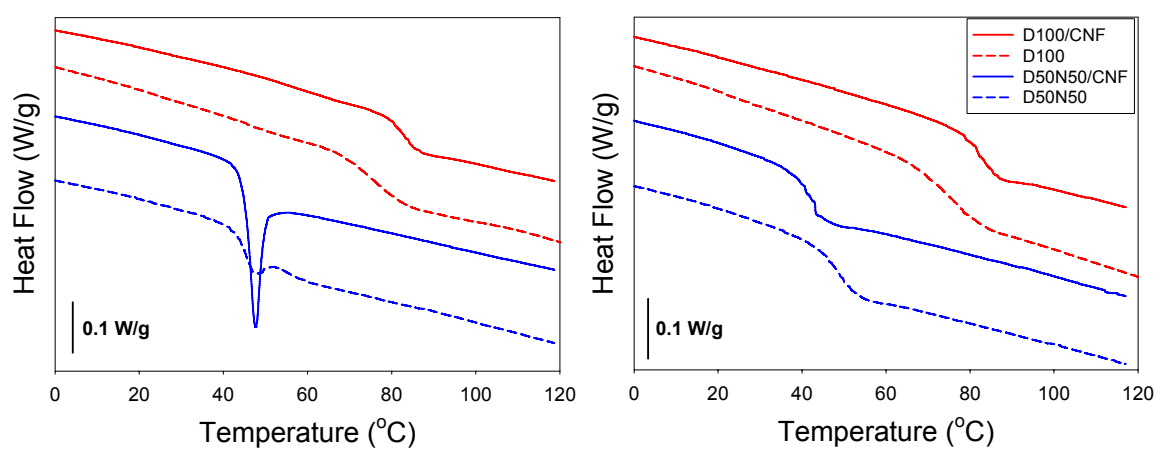


Figure S1. Differential scanning calorimetry (DSC) thermograms (left: 1st heating; right: 2nd heating) of Epoxy/CNF nanocomposites compared with neat epoxy resins. The experiments were conducted on a TA Q200 DSC instrument. All heating/cooling rates were 10 °C/min.

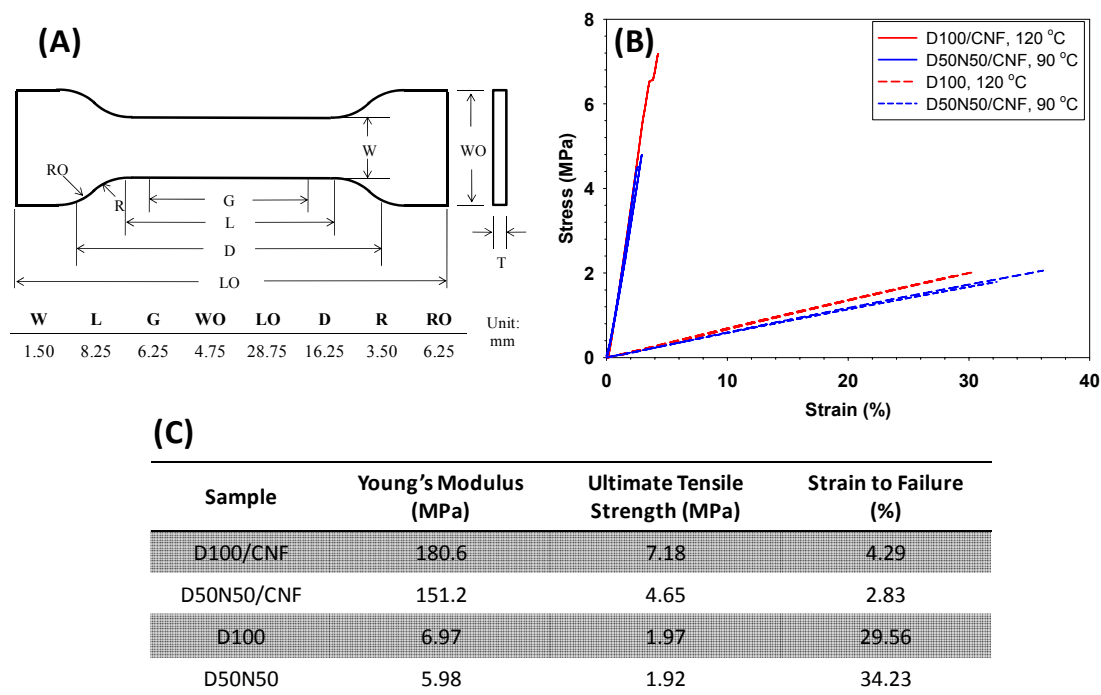


Figure S2. Tensile stress-strain tests of Epoxy/CNF nanocomposites and neat epoxy resins, conducted above the materials' T_g 's (120 °C for D100/CNF and D100, 90 °C for D50N50/CNF and D50N50). Samples were first die-cut into dumbbell-shaped specimens with all the dimensions shown in (A). The specimen was then loaded under tension on a TA Q800 dynamic mechanical analyzer and allowed to equilibrate at the prescribed temperature. The specimen was stretched to complete failure at a constant force rate of 0.1 N/min. The raw stress-strain curves are shown in (B), noting that the gauge length, G , was used to calculate the tensile strain ($\epsilon = \frac{\Delta l}{G} \times 100\%$). Table (C) summarizes the mechanical properties (Young's modulus, ultimate tensile strength and strain-to-failure) of the four samples tested.

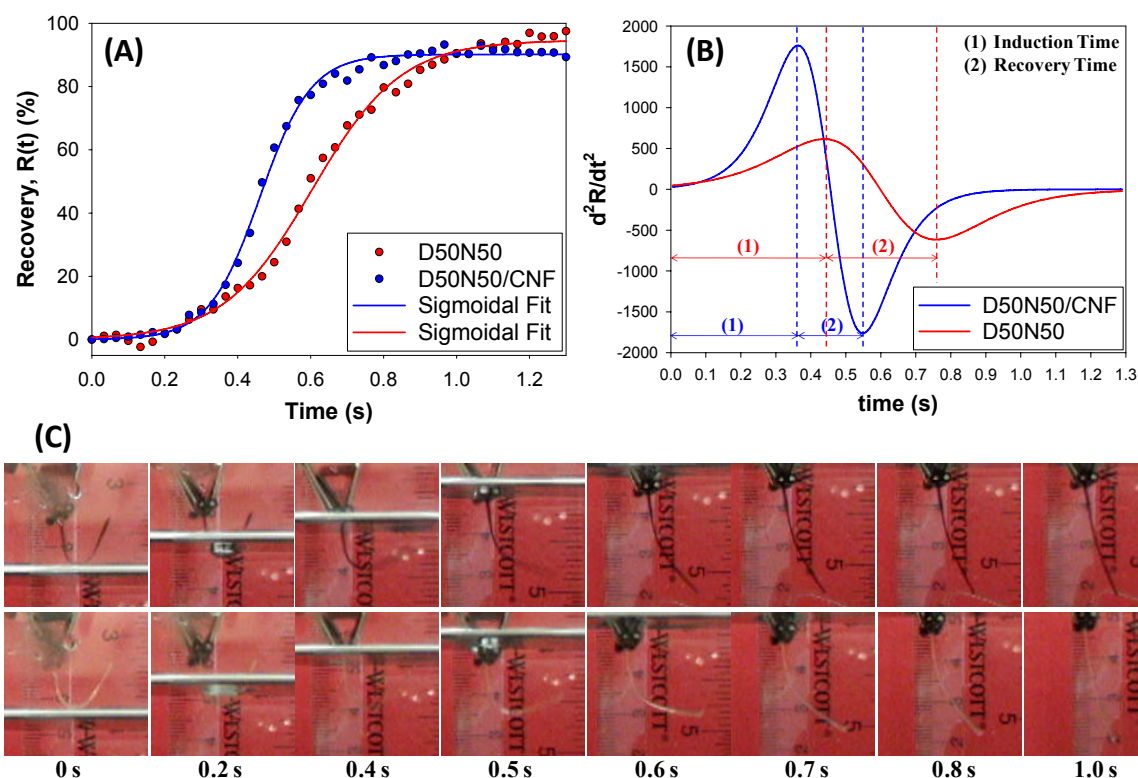


Figure S3. Isothermal shape recovery experiments of D50N50/PCL and D50N50. The dumbbell geometry shown in Fig. S2(A), with a constant thickness of 0.31 mm was used. The sample was first heated above its T_g , quickly deformed by hand to a bent shape and allowed to cool to room temperature for shape fixing. The shape recovery was triggered by immersing the deformed samples into a hot water bath at 60 °C, with digital images taken at a constant frame rate of 30 Hz. The recovery (%) was calculated based on the change of deformation angle during recovery (detailed in the main text). (A) Time-dependent recovery profiles for D50N50/CNF and D50N50, with both data sets fit using a standard 3-parameter sigmoidal function. Two characteristic times were defined using the second derivative plots of the fit functions, as shown in (B). The induction time (time before rapid shape recovery takes place) is the time between zero (when the sample started contacting the water) and the first peak. The recovery time (time taken for the shape recovery, i.e. from onset to completion) is defined as the time interval between the two peaks. From (B) it can be seen that D50N50/CNF recovers much faster than D50N50, in that both the induction time and the recovery time were shortened. As discussed in the main text this is attributed to the increased thermal conductivity due to the incorporation of CNFs. (C) shows the digital images at selected time points for D50N50/CNF (top) and D50N50 (bottom).

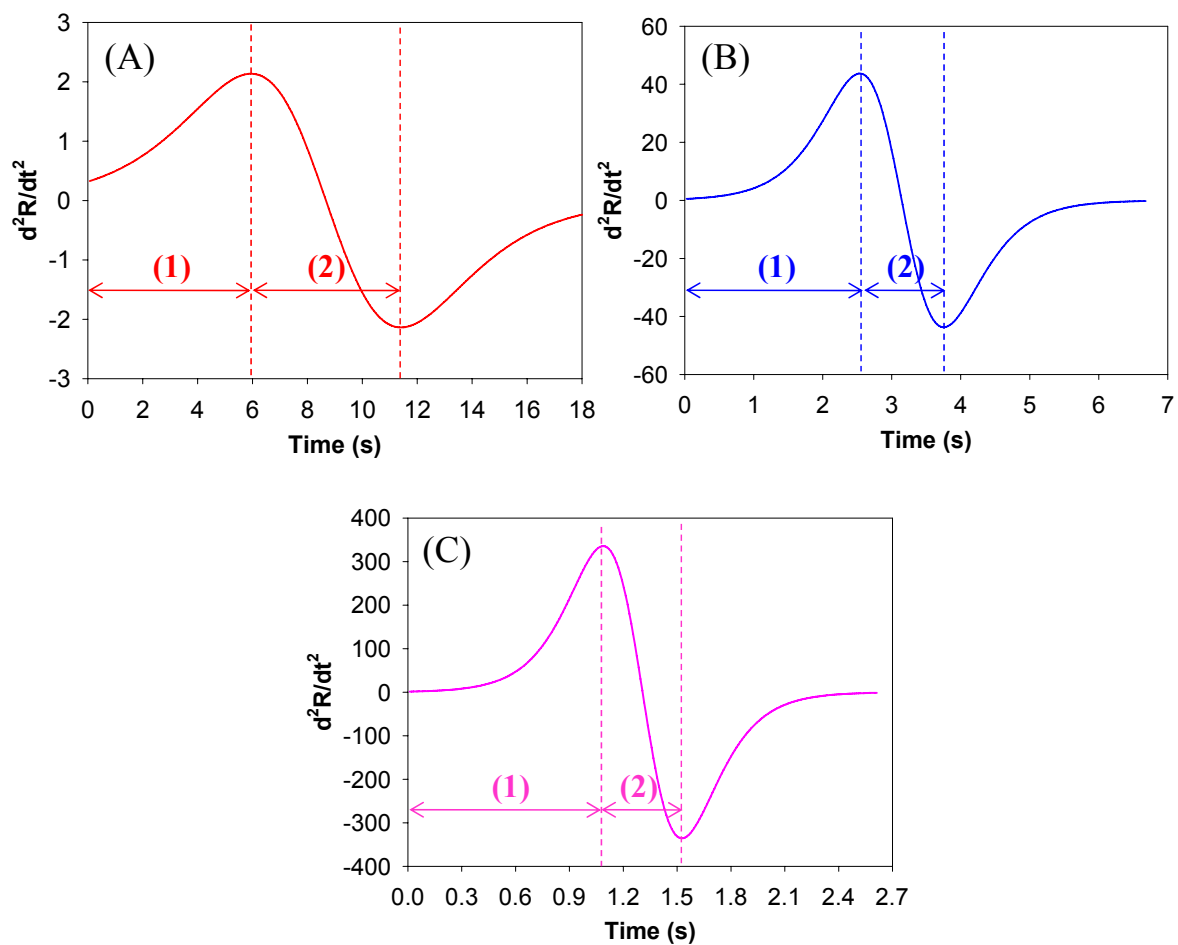


Figure S4. The 2nd time-derivative plots of the fit sigmoidal recovery curves (see Fig. 3B) for D50N50/CNF under different DC voltages of (A) 10 V, (B) 15 V and (C) 20 V. The (1) induction time and (2) recovery time are defined on each graph.

Movie. A movie showing the electrically triggered recovery of D50N50/CNF during application of a DC voltage of 20 V.

A Brief Analysis and Additional Comments on Dimensional Dependence of Recovery Rate

Assuming all the Joule heat from resistive heating is absorbed by the sample, i.e. no convective heat loss:

$$\frac{U^2}{R} dt = C_p m dT \quad (1)$$

Here U , R , C_p , m , t and T are applied DC voltage, sample resistance, heat capacity, sample mass, time and temperature, respectively. For simplicity we neglect the temperature dependence of R and C_p .

For a rectangular film geometry, m and R can be calculated as:

$$m = \rho Al \quad (2)$$

$$R = \frac{rl}{A} \quad (3)$$

where ρ , A , l and r stand for sample density, cross-sectional area, length (along the voltage direction) and electrical resistivity, respectively. Combining (1), (2) and (3) leads to

$$\frac{dT}{dt} = \frac{1}{C_p \rho r} \times \left(\frac{U}{l}\right)^2 \quad (4)$$

The above equation indicates that, geometrically, the electrical heating rate (dT/dt) is only a function of the sample length (rate $\sim l^2$) and electrically is a function of the voltage applied (rate $\sim U^2$).

First we have to mention that, based on our literature search, no author has ever explored (either experimentally or theoretically) dimensional dependence of electrical properties of electro-conductive SMPs; nor is there a “standard” protocol for evaluating shape recovery under DC voltage (this can be seen from Table S1). This is understandable since this is a relatively new field. However based on equation (4) as well as the facts that among all previously reported experiments (a) our applied voltage is the lowest, (b) our sample length (l , approximately 36 mm for our geometry) is comparable to others and (c) our recovery time (< 2 s under 20V) is at least one magnitude smaller, we are confident to conclude that our material has a faster recovery speed than all the existing conductive SMPs with discrete fillers.

Table S1. Comparison of electrically conductive SMPs reported in the literature

Reference	SMP/Filler System	Conductivity, σ (S/m) / Resistivity, ρ (Ω^*m)	Electrically Triggered Recovery Experiment
Leng et al., <i>Appl Phys Lett</i> , 92 , 014104 (2008)	T_g based PU with Ni powders (3-7 μm)	$\sigma = 8.21$ S/m $\rho = 0.1218$ Ω^*m with 10 vol-% Ni (chain direction)	Recovered in 90 s under 20 V (composition unknown)
Leng et al., <i>J Appl Phys</i> , 104 , 104917 (2008)	Thermoset PS with CB (mean aggregate size ~ 4 μm , mean domain size ~ 18 -20 μm) & SCFs (D ~ 7 μm , L ~ 0.5 -3 mm)	$\sigma = 11.22$ S/m $\rho = 0.0891$ Ω^*m with 5 wt-% CB & 2 wt-% SCFs	Recovered in 50 s under 25 V same composition as left
Leng et al., <i>Appl Phys Lett</i> , 92 , 204101 (2008)	T_g based PU with CB (size not known) & Ni powders (3-7 μm)	$\sigma \sim 10$ S/m $\rho \sim 0.1$ Ω^*m with 10 vol-% CB & 2 vol-% Ni	Recovered in 120 s under 30 V same composition as left
Cho et al., <i>Macromol Rapid Comm</i> , 26 , 412 (2005)	PCL based PU with MWCNTs (D ~ 10 -20 nm, L ~ 20 μm)	$\sigma \sim 0.1$ S/m $\rho \sim 10$ Ω^*m with 5 wt-% MWCNTs	Recovered in 10s under 40 V same composition as left
Sahoo et al., <i>Macromol Mater Eng</i> , 290 , 1049 (2005)	PCL based PU with PPY coating	$\sigma = 9.5$ S/m $\rho = 0.105$ Ω^*m with 20 wt-% PPY	Recovered in 25-30 s under 40 V same composition as left
Sahoo et al., <i>Compos Sci Technol</i> , 67 , 1920 (2007)	PCL based PU with PPY (coating or 200-400 nm particles) & MWCNTs	$\sigma = 9.8$ S/m $\rho = 0.102$ Ω^*m with 2.5 wt-% PPY & 2.5 wt-% MWCNTs	Recovered in ~ 20 s under 25 V Same composition as left
Li et al., <i>J Appl Polym Sci</i> , 75 , 68 (2000)	PCL based PU with CB (50-90 nm)	$\sigma = 8.4$ S/m $\rho = 0.119$ Ω^*m with 30 wt-% CB	Not provided
Gunes, et al., <i>Carbon</i> , 47 , 981(2009)	PCL based PU with CB (size not known), CNFs or ox-CNFs (D ~ 60 -200 nm, L ~ 30 -100 μm)	$\sigma \sim 10^3$ S/m $\rho \sim 10^3$ Ω^*m with 7 wt-% CB, CNFs or ox-CNFs	Not provided
Luo and Mather (current work)	Epoxy SMP with <i>continuous</i> non-woven CNFs (D = 135.4 \pm 24.5 nm)	$\sigma = 30.59 \pm 0.81$ S/m $\rho = 0.0327 \pm 0.0008$ Ω^*m with 9.18 \pm 0.33 wt-% (4.72 \pm 0.17 vol-%) CNFs	Recovered in < 2 s under 20 V same composition as left

Abbreviations: PS – polystyrene; PCL – polycaprolactone; PU – polyurethane; CB – carbon black; SCF – short carbon fiber; Ni – nickel; MWCNT – multi-walled carbon nanotube; PPY – polypyrrole; CNF – carbon nanofiber; ox-CNF – oxidized carbon nanofiber; D – diameter; L – length